J|A|C|S
ARTICLES
Published on Web 02/20/2007

From Cd-Rich to Se-Rich − the Manipulation of CdSe Nanocrystal Surface Stoichiometry

Jacek Jasieniak and Paul Mulvaney*

Contribution from the School of Chemistry, University of Melbourne, Parkville, Victoria, 3010, Australia

Received August 30, 2006; E-mail: mulvaney@unimelb.edu.au

Abstract: We report a protocol for manipulating the surface composition of CdSe nanocrystals. By combining the successive ion layer adhesion and reaction (SILAR) method developed by Li et al. *J. Am. Chem. Soc.* **2003**, *125*, 12567 with a phosphine-free selenium precursor, the surface stoichiometry of CdSe can be tunably altered from Cd- to Se-rich. By changing the overall surface stoichiometry, we demonstrate ligand binding to specific surface sites. Tertiary phosphines produce a dramatic enhancement in photoluminescence quantum yield of CdSe particles with Se-rich surfaces but have little effect on Cd-rich surfaces. Unpassivated selenium surface sites are also shown to be a cause of the photobrightening behavior of CdSe nanocrystals.

Introduction

It has long been recognized that appropriate passivation of surface sites is critical for obtaining high luminescence quantum yields from colloidal quantum dots such as CdSe and CdS.[1−5] Nonradiative decay pathways associated with unpassivated surface atoms compete with radiative exciton recombination.[6,7] However, although many different passivants have been found empirically to improve the luminescence quantum yield of semiconductor nanocrystals,[1−3,8] there has been very little work carried out on the more fundamental issue of nanocrystal stoichiometry. In II−VI semiconductors, the valence band is composed primarily of the chalcogenide p orbitals. Theoretical modeling by Leung et al. indicates that the majority of hole traps originate from surface selenium sp^3-hybridized, dangling bond orbitals.[9] Conversely, the conduction band levels are primarily made up from the metal s orbitals, and the empty surface metal ion s orbitals are therefore intrinsic electron traps.[10] There are differing views as to whether the surface trap energies are spread broadly within the band gap, or whether interactions with adsorbates move them closer to the band edges.[11,12] In either case the surface stoichiometry must strongly affect the trapping rates of each charge carrier.

The situation is not symmetric however; in CdSe, there is a fundamental difference between a selenium-rich surface and a cadmium-rich one, which is due to the different stabilities of the electrons and holes within the semiconductor. Valence band holes are thermodynamically unstable within the lattice, and the majority of II−VI binary semiconductors such as CdS and CdSe undergo anodic decomposition.[13−15] For bulk CdSe, this surface process may be written as

$$2h^+ + CdSe \rightarrow Cd^{2+} + Se \qquad E°(\text{NHE}) = +0.35\ \text{V} \quad (1)$$

Since the valence band is located at +1.5 V NHE in aqueous solution,[16] lattice corrosion is inevitable if a free valence band hole is unable to recombine with an electron or to be scavenged by a hole scavenger at the surface. Conversely, however, conduction electrons ($E_{cb} = -0.2$ V NHE) do not initiate cathodic reduction of the lattice. This is because the parallel corrosion reactions of the conduction electrons are thermodynamically unfavorable

$$CdSe + 2e^- \rightarrow Cd° + Se^{2-} \qquad E°(\text{NHE}) = -1.3\ \text{V} \quad (2)$$

Corrosion can be prevented if the surface lattice ions can be properly passivated. For example, in the case of surface cadmium ions on CdSe surfaces, donation of electron density from the lone pair of a ligand leads to formation of a dative bond, which lowers the energy of the ligand lone pair, while raising the energy of the empty 5s orbital above the conduction band rendering the particle photostable (Scheme 1).

Clearly, the ability to passivate the crystal is predicated on control of the surface composition, and the surface stoichiometry of binary semiconductor nanocrystals must play a critical role in the photostability of the semiconductor. Alkylamine or

(1) Talapin, D. V.; Rogach, A. L.; Kornowski, A.; Haase, M.; Weller, H. *Nano Lett.* **2001**, *1*, 207.
(2) Kalyuzhny, G.; Murray, R. W. *J. Phys. Chem. B* **2005**, *109*, 7012.
(3) Bullen, C.; Mulvaney, P. *Langmuir* **2006**, *22*, 3007.
(4) Spanhel, L.; Haase, M.; Weller, H.; Henglein, A. *J. Am. Chem. Soc.* **1987**, *109*, 5649.
(5) Kortan, A. R.; Hull, R.; Opila, R. L.; Bawendi, M. G.; Steigerwald, M. L.; Carroll, P. J.; Brus, L. E. *J. Am. Chem. Soc.* **1990**, *112*, 1327.
(6) Underwood, D. F.; Kippeny, T.; Rosenthal, S. J. *J. Phys. Chem. B* **2001**, *105*, 436.
(7) Bawendi, M. G.; Carroll, P. J.; Wilson, W. L.; Brus, L. E. *J. Chem. Phys.* **1992**, *96*, 946.
(8) Dannhauser, T.; O'Neil, M.; Johansson, K.; Whitten, D.; McLendon, G. *J. Phys. Chem.* **1986**, *90*, 6074.
(9) Leung, K.; Whaley, K. B. *J. Chem. Phys.* **1999**, *110*, 11012.
(10) Hill, N. A.; Whaley, K. B. *J. Chem. Phys.* **1994**, *100*, 2831.
(11) Gomez, D. E.; van Embden, J.; Jasieniak, J.; Smith, T. A.; Mulvaney, P. *Small* **2006**, *2*, 204.
(12) Eychmueller, A. A.; Hässelbarth, A.; Katsikas, L.; Weller, H. *Ber. Bunsen-Ges. Phys. Chem.* **1991**, *95*, 79.
(13) Gerischer, H. *J. Vac. Sci. Technol.* **1978**, *15*, 1422.
(14) Bard, A. J.; Wrighton, M. S. *J. Electrochem. Soc.* **1977**, *124*, 1706.
(15) Memming, R. *J. Electrochem. Soc.* **1978**, *125*, 117.
(16) Nozik, A. J.; Memming, R. *J. Phys. Chem.* **1996**, *100*, 13061.

Scheme 1. Representation of the Interaction between a "Cd" Surface Trap State (Lewis Acid) and a Typical Lewis Base Ligand, i.e., an Aliphatic Amine

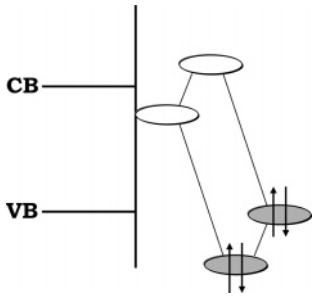

alkylphosphine oxide ligands have been shown to be effective Lewis bases (electron donors), binding to surface Cd sites on both CdSe nanocrystals and bulk samples.[2,3,17,18] Phosphines have been employed as selenium surface site passivants,[7,19] but the mechanism of passivation is unclear. Alkylphosphines may simply act as hole scavengers since they are strong reductants. Alternatively, they may adsorb to Cd vacancies and reduce the rate of electron trapping; they may remove oxygen, which is an effective electron scavenger, or they may indeed chemically passivate surface Se sites.

Since the electrons in surface states are not thermodynamically capable of cathodically decomposing the lattice, they should have a long residence time within the lattice and may be injected back into core exciton states or they may recombine with free or trapped holes.[12] Henglein and co-workers have shown using pulse radiolysis that single electrons may be stable for up to a minute on colloidal CdS, whereas injection of holes leads to immediate loss of luminescence and particle oxidation.[20,21] It is therefore essential not only to identify efficacious passivants but also to understand their effects on charge carrier recombination. As long as both types of surface state are present, there are both electron and hole trapping states to catalyze nonradiative recombination of charge carriers within the QD as well as corrosion of the lattice. Studies of II−VI and III−V semiconductor nanocrystal photochemistry are needed in which there is control of surface stoichiometry. This problem has proved to be simpler to solve for the elemental semiconductors such as Si, which can be passivated by atomic hydrogen only.[22,23] Interestingly, for nonaqueous based syntheses of II−VI nanocrystals, the surface stoichiometry has been found to be rather insensitive to the initial amount of monomer. This has prevented specific tuning of the surface composition in single pot syntheses. In the case of CdSe the Cd/Se ratios of the resulting particles are always found to be between 1 and 1.2 depending on the method of preparation.[24−27] Aqueous studies of CdS have however demonstrated that surface precipitation of cadmium polyphosphate complexes onto CdS leads to enriched Cd surfaces with significantly improved photophysical properties.[4] A similar lyophobic surface manipulation protocol would therefore be useful for studying surface trapping dynamics and surface chemistry and ultimately in optimizing the surface of a core prior to shell deposition.[28−30]

We have recently reported a simple synthesis of CdSe, which obviates the use of any selenium passivant, thus providing a useful reference point for investigating surface stoichiometry and chalcogenide passivation.[31] The phosphine-free solution of Se dispersed in 1-octadecene (ODE-Se) is ideal for growing particles using the recently reported SILAR method and enables submonolayer control of the particle growth. The SILAR technique has already proved to be extremely useful for nanoparticle engineering, and it has been used to prepare the following: core−shell CdSe−CdS QDs;[32] highly stable, graded-seal structures such as CdSe−CdS−$Cd_{1/2}Zn_{1/2}S$−ZnS;[28] and elaborate, multilayer, quantum well structures.[33,34]

In this report, we combine the phosphine-free synthesis with the SILAR approach of Li et al.[32] and Xie et al.[28] in order to prepare a series of CdSe nanocrystals with tunable surface stoichiometries. We find that the introduction of unpassivated Se sites has a drastic effect on the chemical and photochemical properties of semiconductor nanocrystals and that the passivation of these nonradiative chalcogenide sites is critical for obtaining high photoluminescence (PL) and photochemical stability. We show that it is possible to identify the adsorption sites of ligands on such surface-tunable nanocrystals and that this enables the preparation of highly luminescent CdSe nanocrystals with either Cd-rich or Se-rich surfaces. We further demonstrate that the trialkylphosphines that are regularly used in the synthesis of semiconductor nanocrystals can enhance the PL or quench it depending on the surface stoichiometry of the nanocrystal.

Experimental Section

Chemicals. Cadmium oxide (CdO, Aldrich, 99.99%), selenium powder (Aldrich, 99.9%), oleic acid (Aldrich, 90%), trioctylphosphine (TOP, Aldrich, 90%), 1-octadecene (ODE, Aldrich, 90%), octadecylamine (ODA, Merck, 90%), octylamine (Fluka, 98%), hexanethiol (HT, Fluka, 97%), and bis(2,2,4-trimethylpentyl) phosphinic acid (TMPPA, Cytec Specialty Chemicals, 87%) were used in the preparations described here. All solvents used were of analytical grade and purchased from Univar. All chemicals and solvents were used without further purification.

Experimental Details. The nanocrystal preparations were adapted from those recently reported.[31] Briefly CdO (0.08 g, 0.625 mmol) and oleic acid (1.08 g, 3.45 mmol) in 16 g of ODE were heated to 80 °C and degassed for 30 min. The solution was then heated to 310 °C under nitrogen until a colorless solution resulted. At this point a 0.1 M solution of ODE-Se (6.0 g, 0.761 mmol) and TMPPA (1.13 g, 3.39 mmol) was swiftly injected. The growth temperature was set to 235 °C, and

(17) Meyer, G. J.; Lisensky, G. C.; Ellis, A. B. *J. Am. Chem. Soc.* **1988**, *110*, 4914.
(18) Lisensky, G. C.; Penn, R. L.; Murphy, C. J.; Ellis, A. B. *Science* **1990**, *248*, 840.
(19) Kim, S.; Bawendi, M. G. *J. Am. Chem. Soc.* **2003**, *125*, 14652.
(20) Kumar, A.; Henglein, A.; Weller, H. *J. Phys. Chem.* **1989**, *93*, 2262.
(21) Henglein, A. *Chem. Rev.* **1989**, *89*, 1861.
(22) Wilkinson, A. R.; Elliman, R. G. *Phys. Rev. B: Condens. Matter* **2003**, *68*, 155302/1.
(23) Wilkinson, A. R.; Elliman, R. G. *Appl. Phys. Lett.* **2003**, *83*, 5512.
(24) Katari, J. E. B.; Colvin, V. L.; Alivisatos, A. P. *J. Phys. Chem.* **1994**, *98*, 4109.
(25) Dabbousi, B. O.; Rodriguez-Viejo, J.; Mikulec, F. V.; Heine, J. R.; Mattoussi, H.; Ober, R.; Jensen, K. F.; Bawendi, M. G. *J. Phys. Chem. B* **1997**, *101*, 9463.
(26) Taylor, J.; Kippeny, T.; Rosenthal, S. J. *J. Cluster Sci.* **2001**, *12*, 571.
(27) Qu, L.; Peng, X. *J. Am. Chem. Soc.* **2002**, *124*, 2049.
(28) Xie, R.; Kolb, K.; Li, J.; Basché, T.; Mews, A. *J. Am. Chem. Soc.* **2005**, *127*, 7480.
(29) Manna, L.; Scher Erik, C.; Li, L.-S.; Alivisatos, A. P. *J. Am. Chem. Soc.* **2002**, *124*, 7136.
(30) McBride, J.; Treadway, J.; Feldman, L. C.; Pennycook, S. J.; Rosenthal, S. J. *Nano Lett.* **2006**, *6*, 1496.
(31) Jasieniak, J.; Bullen, C.; van Embden, J.; Mulvaney, P. *J. Phys. Chem. B* **2005**, *109*, 20665.
(32) Li, J. J.; Wang, Y. A.; Guo, W.; Keay, J. C.; Mishima, T. D.; Johnson, M. B.; Peng, X. *J. Am. Chem. Soc.* **2003**, *125*, 12567.
(33) Battaglia, D.; Blackman, B.; Peng, X. *J. Am. Chem. Soc.* **2005**, *127*, 10889.
(34) Battaglia, D.; Li, J. J.; Wang, Y.; Peng, X. *Angew. Chem., Int. Ed.* **2003**, *42*, 5035.

Table 1. Reaction Parameters Used during the Surface Modification

reaction parameter	volume of 0.1 M ODE-Se (mL)	total *n*(Se) added (mmol)	Abs λ_{max} (nm)	observed diameter[a] (nm)	as-prepared quantum yield[b] (%)	TOP inclusive quantum yield[b] (%)
Cd1	0.00	0.00	558	3.21	39.9	38.7
Se1	0.231	0.02	565	3.38	38.5	12.6
Se2	0.302	0.05	571	3.55	36.7	6.7
Se3	0.354	0.09	577	3.72	31.6	3.4
Se4	0.354	0.12	583	3.92	27.2	2.8
Se5	0.354	0.16	588	4.10	25.7	4.3
Se6	0.354	0.19	591	4.21	0.24	50.8
Se7	0.354	0.23	592	4.25	0.31	49.3

[a] Based literature values of size vs first absorption peak maxima (Yu et al. ref 36,37). [b] In comparison with R640, with accuracy to within 10%.

growth of the nascent crystallites continued for ~15−20 min. ODA (3 g, 11.1 mmol) was then added to the solution, and the crystals were annealed for 2 h at 180 °C. The resulting NCs were washed via a chloroform−methanol−acetone extraction. Tuning of the NCs surface stoichiometry was performed utilizing a modified SILAR method. 2.24 × 10^{-7} mol of 3.21 nm NCs were degassed in 1.36 g of ODA and 3.24 g of ODE at 80 °C for at least 1 h. The temperature was then slowly ramped up to 225 °C for surface layer growth. 0.1 M stock solutions of ODE-Se and ODE-CdTMPPA (0.8 M TMPPA) were utilized to tune the surface stoichiometry. The first layer to be grown was a full monolayer of Cd (0.2906 mL) forming a Cd-rich surface. An 8-fold excess of oleic acid was included at this stage to aid shell growth. This was followed by the incremental addition of Se. The surface stoichiometry was designed to be tuned from one with excess Cd, to one that was equimolar, and finally to one that was Se-rich. Each selenium addition is designated Se*N*, where *N* is the ODE-Se injection number; i.e., Se1 is the sample following the first injection. The exact quantities of ODE-Se added during each addition are listed in Table 1. For each injection, the growth time was fixed at 10 min. It has been shown that the ODE-Se monomer reactivity is approximately 50%, and therefore some free selenium is always present in solution.[31] Aliquots of the growth solution were extracted following each growth period and diluted immediately with chloroform. For fluorescence and absorption measurements, no postsynthesis washing steps were performed to avoid complications from solvent passivation effects. The addition of passivating agents was made within 1 h of synthesis to minimize the possibility of surface oxidation of the nanoparticles. The steady-state fluorescence spectra presented here were obtained after 1 h of passivation time for hexanethiol (HT) and TOPSe and after 14 h for TOP passivation. When HT or TOPSe were used the samples already had equimolar quantities of TOP in solution, ~5 mM to standardize any competing passivation effects. The fluorescence stability was measured by illuminating samples in a 1 cm cuvette with a 150 W xenon arc lamp equipped with a 0.9 transmission 400 nm cutoff filter. For aerated studies the samples were stirred while open to air, and any evaporated solvent was replenished. Nitrogen purged conditions utilized capped samples that had been bubbled with high purity nitrogen for a minimum of 10 min. For Cd-rich surfaces, we made use of octylamine, oleic acid, and TOP at concentrations of ~5 mM in solution. The errors in the stability measurements reflect the spectrometer resolution (±0.4 nm) and slight changes in PL yield due to temperature fluctuations (±5%). The absorbance at the excitation wavelength for all PL studies was less than 0.10. Quantum yield measurements were performed with reference to Rhodamine 640 in methanol and are accurate to within ±10%.[35] Absorbance and photoluminescence spectra were collected with a Cary 5 UV−vis−NIR spectrometer and a Varian Eclipse, respectively. Samples for XPS were prepared by thoroughly washing the nanocrystals with a combination of extraction (5 times) and precipitation cycles to remove any unbound monomer and then depositing the powder onto carbon tape. XPS was performed on a Kratos Axis Ultra spectrometer using Al Kα excitation. Elemental compositions were calculated from high-resolution spectra of C 1s, O 1s, Se 3d, and Cd 3d photoemission lines with a pass energy of 20 eV. The binding energies were referenced to C 1s at 284.6 eV.

Results and Discussion

1. Cd-to-Se-Rich Surface Stoichiometry. From an initially unknown surface stoichiometry, a monolayer of Cd was grown onto the QD surface. In this step the available Cd lattice vacancies were saturated, and it was assumed that the majority of Se surface sites were also passivated by the cadmium complexes. We term these QDs "Cd-rich". Figure 1 shows the evolution of the Cd-rich CdSe QD absorption spectra during the stepwise addition of Se. A red-shift of the absorbance features was observed during the progressive addition of the Se precursor. Because there was excess Cd present in solution, the slow titration caused both the capping of some of the surface Cd ions with Se and the deposition of further Cd ions from solution. Consequently, there was of necessity some growth of the particles as the surface stoichiometry was tuned. In the inset to Figure 1 the particle diameter is shown after each Se addition step, calculated from the calibration data of Yu et al.[36,37] Approaching the end point in the reaction, the Cd monomer in solution was exhausted and no further growth was observed. Based on the predicted amounts needed for monolayer coverage, nearly two full monolayers of CdSe had been deposited at this point. We term these nanocrystals "Se-rich". Further addition of Se beyond this point led to colloidal instability.

To determine the exact surface stoichiometry at different stages of surface manipulation, XPS was performed on three, well-washed samples with slightly different sizes to those described above: (1) as prepared CdSe (radius ~1.73 nm), (2) Cd-rich (r ~1.72 nm) and (3) Se-rich (r ~2.10 nm). The results obtained from the three samples, which henceforth are designated S1, S2 and S3, respectively, are summarized in Table 2. By comparing the integrated Cd 3d and Se 3d signals, the Cd/Se ratio was determined with an accuracy of ±10%. This involved correcting for the differences in the sensitivity factors of the Cd and Se photoelectrons (see Supporting Information). The determined Cd/Se ratios were 1.16, 1.27, and 0.87 for the S1, S2, and S3 samples, respectively. The Cd 3d spectral region for the three samples is shown in Figure 2a. All the samples show the presence of bulk Cd species, while an additional contribution at 0.76 ± 0.04 eV higher binding energy is observed for S1 and S2. Such a contribution has been previously observed during surface analysis of CdS by Winkler et al. and was assigned to surface Cd species.[38] The Cd 3d spectral region in S3 was almost identical to a bulk reference CdSe sample (see Supporting Information) in both peak position and peak width (~0.85 eV), suggesting that there was a great reduction in surface Cd for S3. Analysis of the Se 3d region, shown in Figure 2b, reveals a surface Se contribution is also present in the "Se-rich" S3 sample but not in S1 or S2. Chalcogenide surface contributions have also been previously observed under

(35) Donegá, C. M.; Hickey, S. G.; Wuister, S. F.; Vanmaekelbergh, D.; Meijerink, A. *J. Phys. Chem. B* **2003**, *107*, 489.
(36) Yu, W. W.; Qu, L.; Guo, W.; Peng, X. *Chem. Mater.* **2003**, *15*, 2854.
(37) Yu, W. W.; Qu, L.; Guo, W.; Peng, X. *Chem. Mater.* **2004**, *16*, 560.
(38) Winkler, U.; Eich, D.; Chen, Z. H.; Fink, R.; Kilkarni, S. K.; Umbach, E. *Phys. Stat. Sol. A* **1999**, *173*, 253.

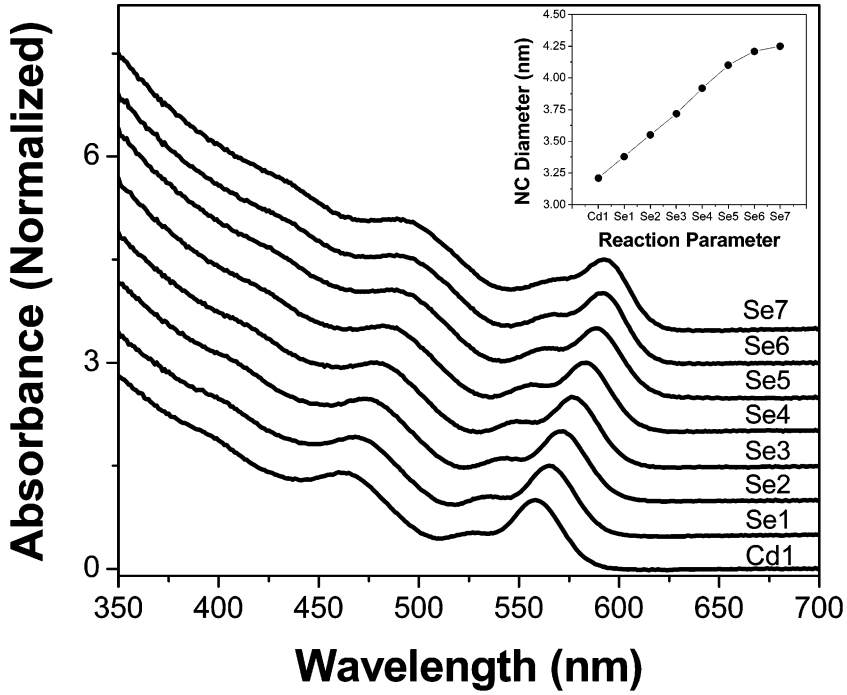

Figure 1. (A) Absorbance spectra taken at different stages of the surface modification in chloroform and (Inset) their respective diameters as determined through known size-absorption dependencies of Yu et al.[36,37]

Table 2. Quantified Atomic Compositions of CdSe NCs with (S1) As-Prepared, (S2) Cd-Rich and (S3) Se-Rich Surface Stoichiometries

	C 1s %	O 1s %	Se 3d %	Cd 3d %	Cd/Se	corrected Cd/Se	surface Cd %	surface Se %
S1	63.65	12.71	10.21	13.43	1.32	1.16	68	32
S2	79.97	8.13	4.88	7.02	1.44	1.27	81	19
S3	86.80	1.86	5.76	5.76	0.97	0.87	30	70

synchrotron irradiation, where low photon energies allowed for improved surface sensitivity.[39,40] Full details of the fitting process and the fitting parameters are included in the Supporting Information.

The XPS data demonstrate that the S1 and S2 samples are Cd-rich, while S3 is Se-rich. We now quantify the surface stoichiometry from these measurements by using a surface saturation model. This model, which is described in more detail in the Supporting Information, assumes that there exists a stoichiometric spherical surface within the nanoparticle and that any excess ions exist on the surface. This is an acceptable assumption as the nanocrystals possess a stoichiometric wurtzite core, and the existence of narrow band-edge PL suggests there are few, if any, point defects within the core.[26,31] For such a surface, the growth of either a selenium or a cadmium layer cannot cause the particle size to increase by more than half a monolayer. Because of this physical limitation we can utilize the known, final particle radius and the experimentally determined Cd/Se ratio to numerically determine the excess coverage needed to satisfy the experimental observations. The results are summarized in Table 2. For S1, S2, and S3, we find the surface Cd(Se) composition to be approximately 68(32)%, 81(19)%, and 30(70)%, respectively, where we define the surface composition as the number of surface Cd or Se species divided by the total number of surface Cd and Se atoms.

The results indicate that the as-prepared particles have a cadmium-rich surface with a stoichiometry that is very similar to those found in previous studies of surface composition on as-prepared CdSe nanoparticles.[6,26] An interestingly corollary is that the limiting nanocrystal stoichiometry is reached when there is a ~70−80% surface coverage of the excess component. This may ultimately reflect the fact that, in a real crystal, facets exist and adsorbates will not bind to all free sites such as vertices and kinks.

2. Luminescence Behavior. (i) Effect of Surface Stoichiometry. In Figure 3a the relative PL intensities for CdSe samples varying from Cd-rich to Se-rich are shown. A gradual decrease in the PL intensity was observed with the addition of selenium up to Se5. This is consistent with an increase in the number of unpassivated surface Se atoms. Interestingly, further addition of Se beyond Se5 led to a drastic decrease in the observed PL intensity by almost 2 orders of magnitude. This sudden decrease was not accompanied by a significant change in particle size or peak broadening, eliminating the possibility that particle aggregation was the cause of the luminescence quenching. The surface stoichiometry at Se6 was "Se-rich" with ~70% of the surface atoms being Se atoms.

(ii) Effect of Trioctylphosphine. Figure 3b shows the resulting PL spectra 14 h after introduction of TOP into CdSe nanocrystal solutions with varying surface stoichiometries. In the inset to Figure 3b we present the quantum yields of the diluted samples removed at different stages of the SILAR reaction, with and without added TOP. The ratio of added TOP molecules to surface selenium atoms was greater than 100 to ensure that all potential adsorption sites were occupied. TOP was found to have little effect on the PL intensity of Cd-rich particles since the Cd surface was already passivated by amine

(39) Adam, S.; McGinley, C.; Moeller, T.; Talapin, D. V.; Borchert, H.; Haase, M.; Weller, H. *Eur. Phys. J. D* **2003**, *24*, 373.
(40) Winkler, U.; Eich, D.; Chen, Z. H.; Fink, R.; Kilkarni, S. K.; Umbach, E. *Chem. Phys. Lett.* **1999**, *306*, 95.

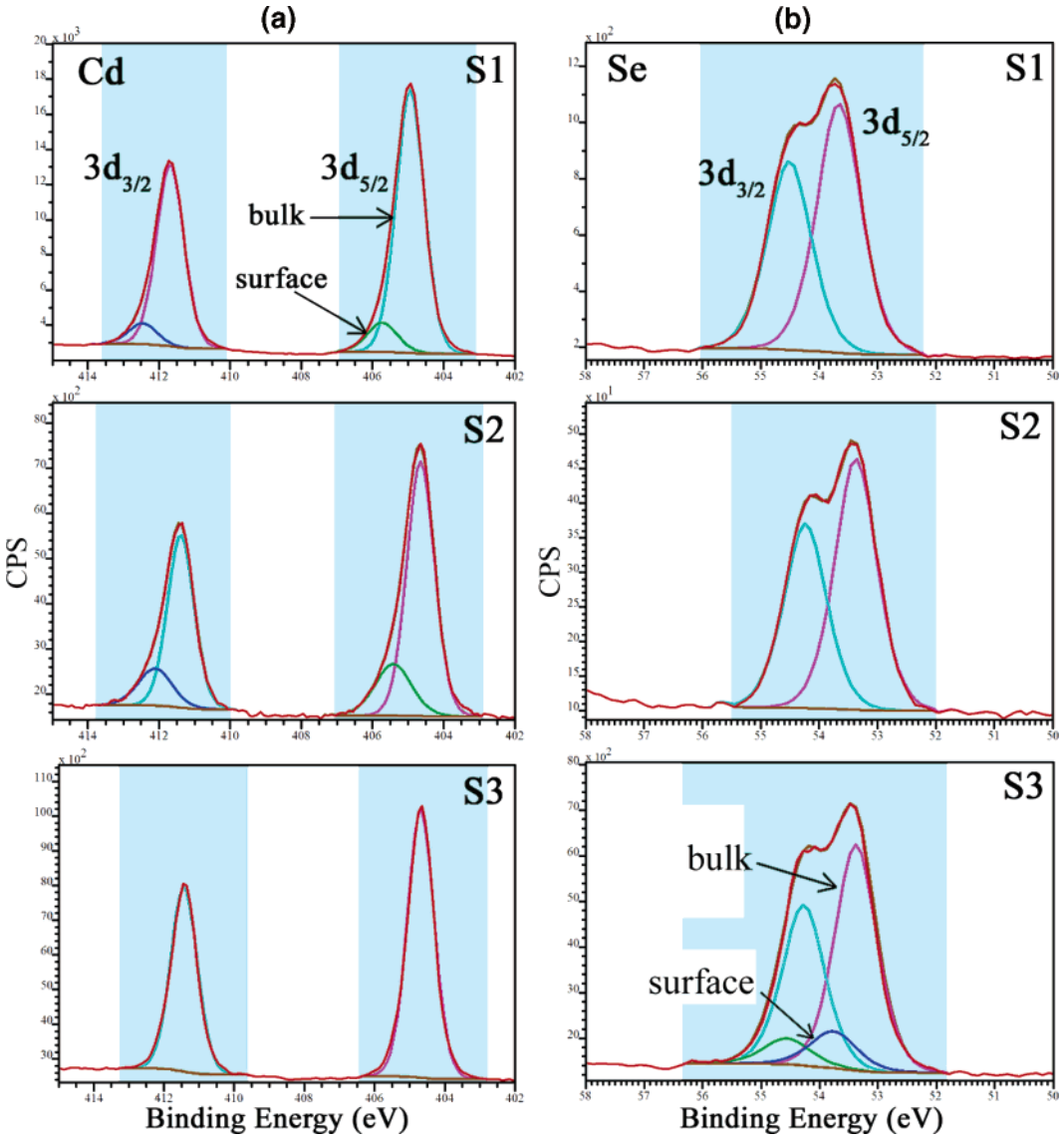

Figure 2. X-ray photoelectron spectra of Cd 3d (a) and Se 3d (b) regions for CdSe nanocrystals with as-prepared (S1), Cd-rich (S2) and Se-rich (S3) surface stoichiometries. Peak analysis utilizing Voight lineshapes show well-defined bulk and surface contributions in the experimental data.

ligands. Either TOP does not complex surface Cd ions or its binding constant is much smaller than that of alkylamines. Experiments in the absence of alkylamines could not be carried out because of particle aggregation. In direct contrast, a staggering 200-fold increase in PL was observed when Se-rich particles were TOP treated. The PL of TOP passivated, Se-rich particles rose to ~10% higher than that of the amine passivated, Cd-rich sample. (We note that the extent of the TOP effect did vary for different nanocrystal samples, but in general the final QY ranged between 40 and 55%.) These results demonstrate that TOP selectively passivates selenium surface states and that selenium trap sites play an integral role in determining the PL quantum yields of CdSe QDs.

The intermediate surface stoichiometry region is complicated, and the results appear to be a convolution of two different processes: (1) passivation and (2) quenching. The passivation process involves the removal of surface selenium trap sites as described above, which enhances the PL. The second, the quenching effect, appears to involve a byproduct of the TOP addition. To determine the nature of this product, ^{31}P NMR spectra were collected on a sample in which TOP was added into a solution of ODE-Se at room temperature and allowed to react for 14 h under ambient conditions (Supporting Information, Figure S1). The NMR data revealed that within this time TOP both partly oxidized to form TOPO and also partly reacted with the Se to form TOPSe. It is known that TOPSe binds to surface Cd atoms in an analogous fashion to TOPO.[41] However, in contrast to TOPO, TOPSe has been shown to quench the PL of CdSe nanocrystals.[2,41] Consequently, the effects of TOP on the luminescence of CdSe nanocrystals is critically dependent on the surface stoichiometry. On a Se-rich surface, TOP passivates hole traps and the luminescence is drastically enhanced. However for nanocrystals which exhibit both Se and Cd surface sites, the TOP will passivate the Se sites, while TOPSe will quench the luminescence by adsorbing to the Cd surface sites. The overall effect on PL depends on the relative concentrations of TOP, free selenium, and the surface stoichiometry.

(iii) Effect of TOPSe and Hexanethiol. In Figure 4 we present the relative changes in PL of Cd-rich CdSe NCs and TOP-activated, Se-rich NCs following addition of TOP, TOPSe,

(41) Rafeletos, G.; Nørager, S.; O'Brien, P. *J. Mater. Chem.* **2001**, *11*, 2542.

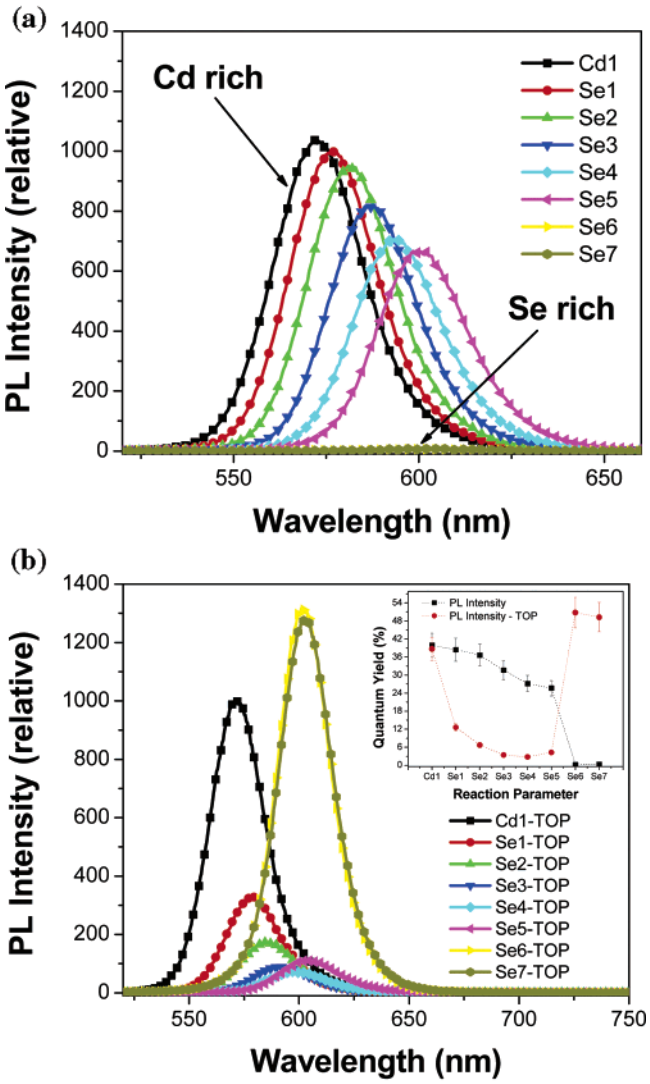

Figure 3. (A) Photoluminescence of the "as-prepared" CdSe nanocrystals at different stages of the surface modification. (B) Photoluminescence of "TOP-activated" nanocrystals. In the inset of (B) a comparison of the relative quantum yields of the "as-prepared" and "TOP-activated" nanocrystals measured against Rhodamine 640 is given within an accuracy of ±10%. (C) Photo of the Cd1, Se1, and Se1-TOP nanocrystals under ambient light and under UV excitation (peak at 360 nm).

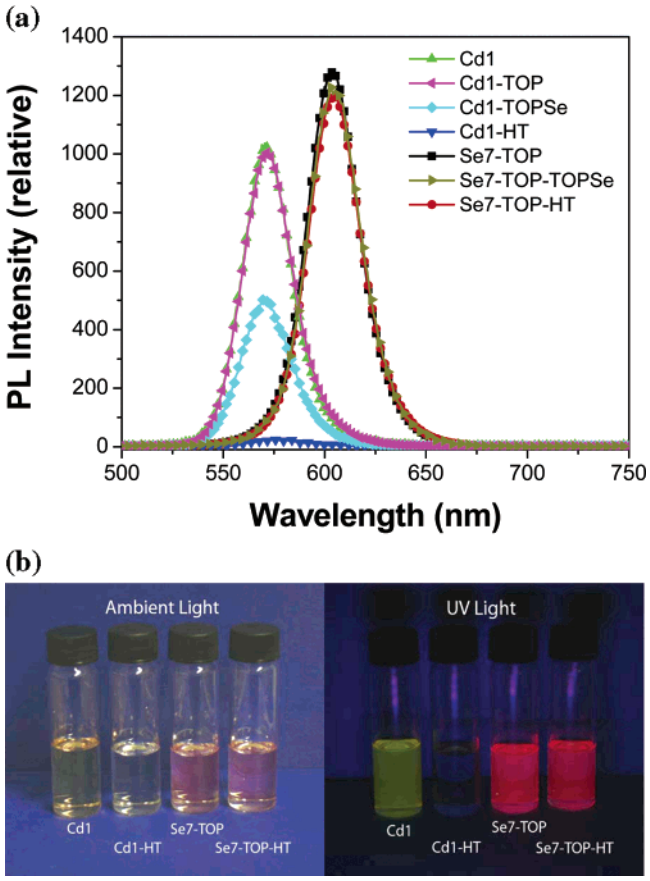

Figure 4. (A) Effect of ligand passivation on the relative nanocrystal photoluminescence of Cd1 and Se7-TOP samples. For both hexanethiol and TOPSe passivation of the Cd1 sample, ~5 mM TOP was included in solution to ensure similar ligand conditions for both surface types. (B) Photo of Cd1 and Se7-TOP samples before and after hexanethiol (HT) passivation under both ambient and UV light.

and a hole acceptor, hexanethiol (HT). Excess TOP was present in both the Cd-rich and Se-rich samples during the addition of other passivants. While TOP itself had very little effect on Cd-rich particles, both TOPSe and HT caused a large decrease in the PL intensity. In direct contrast to the cadmium-rich particles, TOP-activated, Se-rich particles exhibited almost no PL dependence on TOPSe or HT addition. This result clearly demonstrates the dramatic differences in the chemical nature of Cd- and Se-rich CdSe nanocrystals. The Se-rich particles have limited available Se vacancies, which are the binding sites for mercaptans on CdSe.[42] The insensitive (sensitive) nature of a Se(Cd)-rich surface toward TOPSe supports the hypothesis that the behavior of CdSe nanocrystals with intermediate surface stoichiometries is due to the competition between TOP passivation and TOPSe quenching. Although it is very difficult to decouple the extent of each process, it is evident that quenching by TOPSe will dominate over passivation by TOP for Cd-rich surfaces (i.e., Se1−Se3), while the opposite process dominates for Se-rich surfaces (Se4−Se7). Incidentally, no quenching was observed when TOP was added into the Cd-rich solution (Cd1) as there was no available Se monomer in solution, and hence TOPSe formation did not occur.

3. Surface Trapping, Photobrightening, and Stability. We now focus on the photostability of CdSe nanocrystals with different surface compositions. Figure 5 shows the effect of illuminating a Se-rich CdSe colloid under a nitrogen atmosphere. The Se-rich QDs, which originally exhibited ~0.15% PL QY, underwent dramatic photobrightening in the first 120 min of irradiation. Within this time the PL increased by ~2 orders of magnitude (up to a QY of ~15%) with an associated spectral blue-shift of ~1 nm. After peaking at 120 min, the PL emission

(42) Berrettini, M.; Braun, G.; Hu, J. G.; Strouse, G. F. *J. Am. Chem. Soc* **2004**, *126*, 7063.

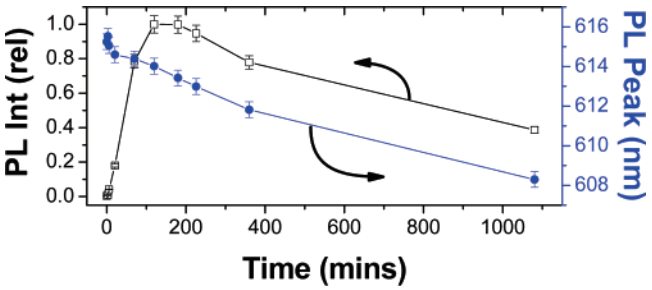

Figure 5. Change in the PL intensity (□) and peak position (●) of a Se-rich sample under illumination in a nitrogen-purged environment.

intensity gradually decreased and a steady blue-shift in the PL peak was observed for the remainder of the experiment. In Figure 6a and b the results are shown of irradiating a TOP-activated, Se-rich CdSe solution in air and under nitrogen, respectively. In both environments photobrightening was observed, with the enhancement in air being ∼25% higher than that when under nitrogen. Following this enhancement, both samples exhibited photodarkening. For the aerated sample, the PL decreased by ∼95% over the first 180 min. In contrast, following an initial, slow decrease in luminescence, the nitrogen purged CdSe colloid showed significantly higher overall stability. The PL peak positions for both samples underwent an initial red-shift. The aerated sample then began to exhibit dissolution, while the sample under nitrogen was photostable. To illustrate the effect of air, the nitrogen purged sample was exposed to an aerated environment following 1500 min of illumination. Within 100 min the sample exhibited a decrease in PL of ∼94% with respect to the value recorded at 1500 min. Particle dissolution occurred simultaneously.

A number of studies have already discussed photobrightening,[29,43−50] and many causes have been invoked including oxidation of Se surface sites, photoinduced passivation by water, and surface reconstruction. Our data strongly suggest that unpassivated Se surface sites are responsible for large photobrightening events. Following the initial photobrightening stage, both TOP-activated and unactivated Se-rich particles underwent photodarkening. However, only the unactivated particles underwent significant dissolution. This reflects the efficient passivation of hole traps by the phosphine in TOP-activated particles.

In the case of the activated samples, a large excess of TOP (∼5 mM) was initially introduced into the solution, but TOP is known to react quickly in the presence of dissolved oxygen (1−10 mM range in aerated solution) to form TOPO (2 TOP + O_2 → 2 TOPO), even in the dark. The TOP therefore passivates the Se-rich surface and also acts as a mild antioxidant but ultimately does not prevent dissolution in aerated conditions once all of the TOP is oxidized.

The effects of illumination on amine-passivated, Cd-rich QDs are shown in Figure 7a and b for aerated and nitrogen-purged environments, respectively. No photoenhancement was observed for either sample. In the case of QDs in an aerated environment, significant photoinstability was observed. The PL decreased to 10% of the initial value in the first 65 min, with an associated 4 nm blue-shift of the luminescence peak wavelength, after which the PL stopped decreasing and the size distribution broadened. For the nitrogen-purged nanocrystals, both the PL intensity and peak position were found to be incredibly stable, with only a 1 nm blue-shift after prolonged illumination. Exposing this sample to air led to immediate and rapid particle dissolution, the size distribution broadened, and the PL intensity decreased drastically. We note that the overall photostability did depend on the concentration of amine or carboxylate ligands present in solution. For well-washed samples with minimal free ligand, slightly higher PL instability was observed with little dissolution. In contrast, for solutions rich in the free metal binding ligands we found that significant dissolution was observed if the ligand to surface site ratios were larger than ∼10 000:1. This instability is most likely due to the formation free Cd^{2+} complexes. Overall, the Cd-rich particles exhibit much higher, overall photostability under nitrogen than those that are Se-rich.

Finally we note that Talapin et al.[50] performed photostability measurements on aqueous, polydisperse CdTe ensembles. They

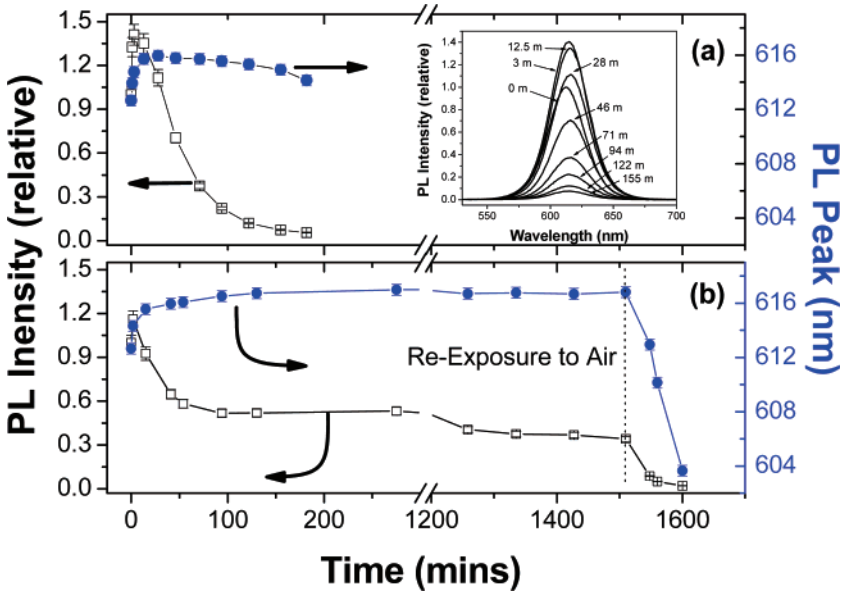

Figure 6. Change in PL intensity (□) and peak position (●) of a TOP-activated Se-rich sample under illumination in (a) an aerated and (b) a nitrogen-purged environment. The inset shows the relative PL spectra at different times of the illumination in an aerated environment.

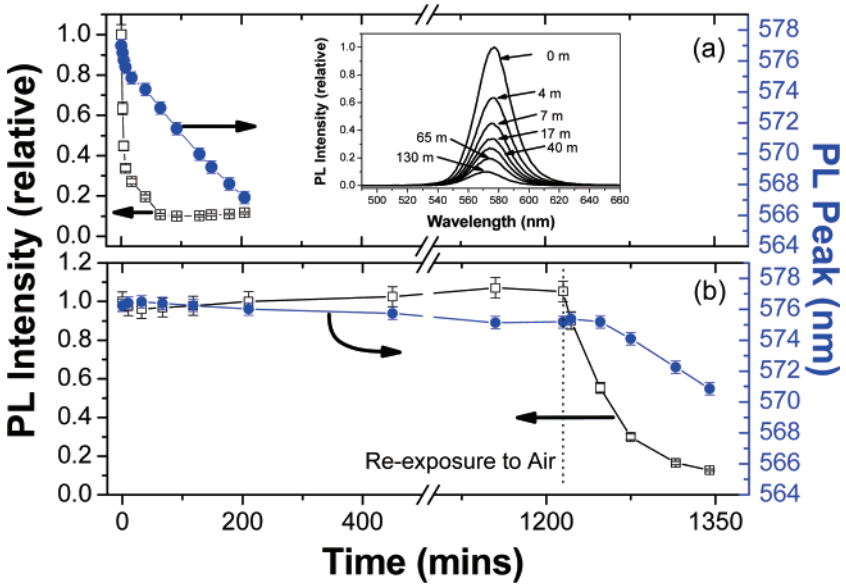

Figure 7. Change in PL intensity (□) and peak position (●) of a Cd-rich sample under illumination in (a) an aerated and (b) a nitrogen-purged environment. The inset shows the relative PL spectra at different times of the illumination in an aerated environment.

showed that within a given ensemble, high and low PL fractions existed. Of these only the low PL fractions exhibited photoenhancement under inert conditions, and the dynamics strongly resembled those of the unpassivated Se-rich particles described here. The high PL fractions did exhibit slightly different dynamics to those shown here; however they are more representative of a Cd-rich stoichiometry as depicted by their high stability under an inert atmosphere. This suggests that within any polydisperse ensemble, various surface stoichiometries are present, and this leads to variations in PL intensity within an ensemble of CdSe nanocrystals.

Conclusions

In this study we have made use of the SILAR protocol to manipulate the surface stoichiometry of CdSe NCs from Cd-rich to Se-rich. The surface contributions were quantified as being ~81% cadmium for Cd-rich and ~70% selenium for Se-rich surfaces. It was determined that particles with different surface stoichiometries have quite different passivation requirements. For particles with an unpassivated, selenium-rich surface, quantum yields less than 0.3% were observed. Through passivation by tri-*n*-octylphosphine, the luminescence quantum yield of Se-rich particles could be drastically increased up to ~50%. Furthermore we showed that the PL properties of TOP "activated" Se-rich QDs are much less sensitive to typical metal binding ligands. Through appropriate surface passivation, it is therefore possible to obtain CdSe particles with quantum yields over 40% with either metal-rich or chalcogenide-rich surfaces. Under oxygen-free conditions, well-passivated Cd-rich surfaces exhibited much better PL stability than those with Se-rich surfaces. While both samples showed instability under aerated conditions, only the Se-rich surfaces exhibited an increase in the observed PL, i.e., photobrightening. In summary, although these results confirm the inherent instability of CdSe in oxidizing environments, the luminescence quantum yields, and the photobrightening are determined primarily by the surface stoichiometry and by the resultant selective surface adsorption of passivants.

Acknowledgment. J.J. thanks the Australian Research Council for postgraduate funding through the APA scheme, and P.M. acknowledges support under the Federation Fellowship program FF0561486. They also acknowledge the invaluable help of Dr. C. Bullen and J. van Embden during the preparation of this manuscript as well as Dr. G. van Riessen and M. Jasieniak for help with the XPS analysis. The work was carried out under ARC DP Grant 0451651.

Supporting Information Available: Correction factor calculations for XPS, bulk CdSe XPS spectra, peak analysis information for Cd and Se 3d regions, surface saturation calculations, and P^{31} NMR results of TOP in ODE-Se solution. This material is available free of charge via the Internet at http://pubs.acs.org.

JA066205A

(43) Wang, Y.; Tang, Z.; Correa-Duarte, M. A.; Pastoriza-Santos, I.; Giersig, M.; Kotov, N. A.; Liz-Marzan, L. M. *J. Phys. Chem. B* **2004**, *108*, 15461.
(44) Jones, M.; Nedeljkovic, J.; Ellingson, R. J.; Nozik, A. J.; Rumbles, G. *J. Phys. Chem. B* **2003**, *107*, 11346.
(45) Myung, N.; Bae, Y.; Bard, A. J. *Nano Lett.* **2003**, *3*, 747.
(46) Wang, Y.; Tang, Z.; Correa-Duarte, M. A.; Liz-Marzan, L. M.; Kotov, N. A. *J Am. Chem. Soc.* **2003**, *125*, 2830.
(47) Nazzal, A. Y.; Wang, X.; Qu, L.; Yu, W.; Wang, Y.; Peng, X.; Xiao, M. *J. Phys. Chem. B* **2004**, *108*, 5507.
(48) Asami, H.; Abe, Y.; Ohtsu, T.; Kamiya, I.; Hara, M. *J. Phys. Chem. B* **2003**, *107*, 12566.
(49) Cordero, S. R.; Carson, P. J.; Estabrook, R. A.; Strouse, G. F.; Buratto, S. K. *J. Phys. Chem.* **2000**, *104*, 12137.
(50) Talapin, D. V.; Rogach, A. L.; Shevchenko, E. V.; Kornowski, A.; Haase, M.; Weller, H. *J. Am. Chem. Soc.* **2002**, *124*, 5782.